DALTON
FULL PAPER

Syntheses, structures and magnetic properties of three-dimensional co-ordination polymers constructed by dimer subunits

Bai-Wang Sun, Song Gao,* Bao-Qing Ma, De-Zhong Niu and Zhe-Ming Wang

State Key Laboratory of Rare Earth Materials Chemistry and Applications, Peking University–The University of Hong Kong Joint Laboratory on Rare Earth Materials and Bioinorganic Chemistry, Peking University, Beijing 100871, P. R. China. E-mail: gaosong@pku.edu.cn

Received 12th July 2000, Accepted 6th September 2000
First published as an Advance Article on the web 19th October 2000

The crystal structures and magnetic properties of compounds $[M^{II}(apo)(N(CN)_2)_2]$, where M = Co (**1**), Ni (**2**) or Mn (**3**), apo = 2-aminopyridine *N*-oxide, have been determined. The structural analyses revealed that they are isomorphous, and all belong to monoclinic space group $P2_1/n$. The metal(II) ions display distorted octahedral co-ordination, with four terminal N atoms of different $[N(CN)_2]^-$ ligands and two O atoms of different apo ligands. Two ions are bridged by two μ-O atoms to form a dimer subunit. Those dimers are further linked to each other by $[N(CN)_2]^-$ resulting in a three-dimensional structure. The magnetic properties of the compounds were investigated in the temperature range 2–300 K for **1** and **2** and 4–300 K for **3**. The values for the intradimer spin coupling constant *J* were estimated to be −17.8, −40, −1.3 cm^{-1} for **1**–**3**, respectively, indicative of antiferromagnetic interaction.

Introduction

The experimental results obtained on the complexes of dicyanamide, $[N(CN)_2]^-$, in the last two years[1–4] are surprisingly rich from both fascinating structural and magnetic points of view. The ligand $[N(CN)_2]^-$ is a remarkably versatile building block for the construction of supramolecular architectures since it may act in a uni-, bi- and tri-dentate manner. Many extended co-ordination polymers have been reported, for example 3-D for $M^{II}[N(CN)_2]_2$ (M = Cu, Co, Ni or Mn),[2,3] 2-D for $Zn[N(CN)_2]_2$[5] and 1-D for $[Mn(N(CN)_2)_2\cdot 2(py)]$ and $[Mn(N(CN)_2)_2](DMF)_2]$.[6] Some of them display unusual magnetic properties including long-range ferromagnetic ordering and hard magnetic behavior. In order to provide more examples for extensive study of the mechanism of magnetic interaction through the bridge $[N(CN)_2]^-$, we have used additional ligands such as *N*-oxides and amines in combination with $[N(CN)_2]^-$ and obtained many complexes with fascinating structures. Here, we report the crystal structure and magnetic properties of three new 3-D co-ordination polymers with formula $[M^{II}(apo)(N(CN)_2)_2]$ (M = Co **1**, Ni **2** or Mn **3**, apo = 2-aminopyridine *N*-oxide), where the dicyanamide anion bridges the metal ions in an end-to-end fashion ($\mu_{1,5}$) and the *N*-oxide apo also bridges. To our knowledge, other examples containing both $\mu_{1,5}$-bonded dicyanamide and co-ligand are only low dimensional complexes except for 3-D α-$[Cu(N(CN)_2)_2(pyz)]$ (pyz = pyrazine)[7] which contains two interpenetrating α-Po-like networks, therefore $[M^{II}(apo)(N(CN)_2)_2]$ represents the first example of dicyanamide complexes with 3-D structure constructed by dimers. This type of extended 3-D structure was also observed in, *e.g.*, $[Cu_3(TMA)_2(H_2O)_3]_n$[8] (TMA = benzene-1,3,5-tricarboxylate).

Experimental

Synthesis

All reagents were commercial grade materials, used as received. $Na[N(CN)_2]_2$ was purchased from Aldrich Company.

$[Co(apo)(N(CN)_2)_2]$ 1. In a small flask apo·HCl (29.32 mg, 0.2 mmol) was dissolved in water (5 mL). The solution was neutralized with a solution of NaOH (1 M). A solution of $CoCl_2\cdot 6H_2O$ (47.59 mg, 0.2 mmol) in water (5 mL) was added, followed by a water solution (5 mL) of $Na[N(CN)_2]$ (35.6 mg, 0.4 mmol). Well shaped mauve polyhedral crystals of $[Co(apo)(N(CN)_2)_2]$ were obtained from the mother liquor by slow evaporation at room temperature for two weeks. They were filtered off, washed with a small amount of water, and dried in air. Yield 65%. Calc. for $C_9H_6CoN_8O$: C, 35.93; H, 2.01; N, 37.21. Found: C, 35.75; H, 2.35; N, 37.11%. Infrared spectrum: $[N(CN)_2]^-$, ν_{sym}(C≡N) 2187, ν_{asym}(C≡N) 2252, ν_{sym}(C–N) 900, ν_{asym}(C–N) 1371; apo bridge, ν(N–H) 3442, ν(N→O) 1204 cm^{-1}.

$[Ni(apo)(N(CN)_2)_2]$ 2. The compound was synthesized as **1** but from $NiCl_2\cdot 6H_2O$ as green crystals. Yield 72%. Calc. for $C_9H_6N_8NiO$: C, 35.93; H, 2.01; N, 37.24. Found: C, 35.68; H, 2.42; N, 37.53%. IR: $[N(CN)_2]^-$, ν_{sym}(C≡N) 2190, ν_{asym}(C≡N) 2256, ν_{sym}(C–N) 935, ν_{asym}(C–N) 1357; apo, ν(N–H) 3440, ν(N→O) 1203 cm^{-1}.

$[Mn(apo)(N(CN)_2)_2]$ 3. The compound was synthesized as **1** but from $MnCl_2\cdot 6H_2O$ as colorless crystals. Yield 76%. Calc. for $C_9H_6MnN_8O$: C, 36.38; H, 2.04; N, 37.71. Found: C, 36.14; H, 1.99; N, 37.31%. IR: $[N(CN)_2]^-$, ν_{sym}(C≡N) 2174, ν_{asym}(C≡N) 2241, ν_{sym}(C–N) 932, ν_{asym}(C–N) 1361; apo, ν(N–H) 3444, ν(N→O) 1206 cm^{-1}.

Physical measurements

Elemental analyses (C, H, N) were carried out by using a Germen Elementar Vario EL instrument. The IR spectra were recorded on a Nicolet Magna-IR 750 spectrometer as KBr pellets in the 4000–400 cm^{-1} region. Magnetic susceptibility data of complexes **1** and **2** were measured by using an Oxford MagLab2000 magnetometer in the temperature range 2–300 K with an applied field of 10 kOe; those of **3** by a Quantum Design MPMS-7 SQUID magnetometer in the range 4–300 K with an applied field of 5 kOe. Diamagnetic corrections were estimated from Pascal's constants.

Crystal data collection and refinement

The structures of compounds **1**, **2** and **3** were studied at Nonius B. V. Demo Lab in Peking University. Data were collected on

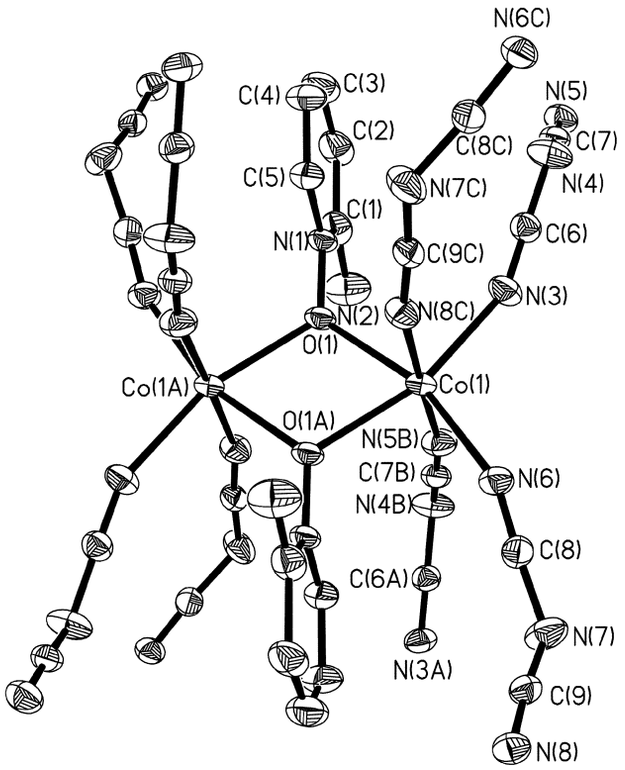

Fig. 1 ORTEP[10] and atom labeling diagram for $[Co(apo)(N(CN)_2)_2]$. Thermal ellipsoids are shown with 30% probability.

a Nonius KappaCCD diffractometer with graphite monochromated Mo-Kα radiation ($\lambda = 0.71073$ Å). The analyses show the compounds are isomorphous. Crystal data are summarized in Table 1. The structures were solved by direct methods followed by Fourier-difference syntheses (SHELXL 97).[9] All non-hydrogen atoms were refined anisotropically, while all hydrogens were assigned to calculated positions.

CCDC reference number 186/2177.

See http://www.rsc.org/suppdata/dt/b0/b005612j/ for crystallographic files in .cif format.

Results and discussion

Selected bond distances and bond angles for $[Co(apo)(N(CN)_2)_2]$ **1**, $[Ni(apo)(N(CN)_2)_2]$ **2** and $[Mn(apo)(N(CN)_2)_2]$ **3** are given in Tables 2, 3 and 4, respectively. The structures of the three complexes are virtually identical, and are exemplified by $[Co(apo)(N(CN)_2)_2]$.

Complex $[Co(apo)(N(CN)_2)_2]$ 1

The cobalt(II) ions display distorted octahedral co-ordination, with the two terminal N atoms of different $[N(CN)_2]^-$ ligands (Co(1)–N(3) 2.074(2); Co(1)–N(6) 2.097(2) Å) and two O atoms of different apo ligands (Co(1)–O(1) 2.144(2); Co(1)–O(1A) 2.114(2) Å) in the equatorial plane, while the other two N atoms of two different $[N(CN)_2]^-$ ligands (Co(1)–N(5B) 2.121(3); Co(1)–N(8C) 2.134(2) Å) occupy the axial positions. They are bridged by two μ-O atoms from two apo to form a dimer subunit. A fragment of the dimer with the atom numbering is shown in Fig. 1. Those dimers are further linked by $[N(CN)_2]^-$ resulting in 3-D structure, each dimer being linked to eight others through $[N(CN)_2]^-$ $\mu_{1,5}$ bridges. Each $[N(CN)_2]^-$ is co-ordinated to two metal atoms *via* the two nitrile nitrogens. The dimer has a centrosymmetric structure with a center of inversion at the middle of the Co_2O_2 plane. The intradimer distance between two cobalt atoms Co(1)···Co(1A) was 3.449(1) Å with a bridge angle (Co(1)–O(1)–Co(1A)) of 108.16(7)°, which is within the range found for similar compounds containing

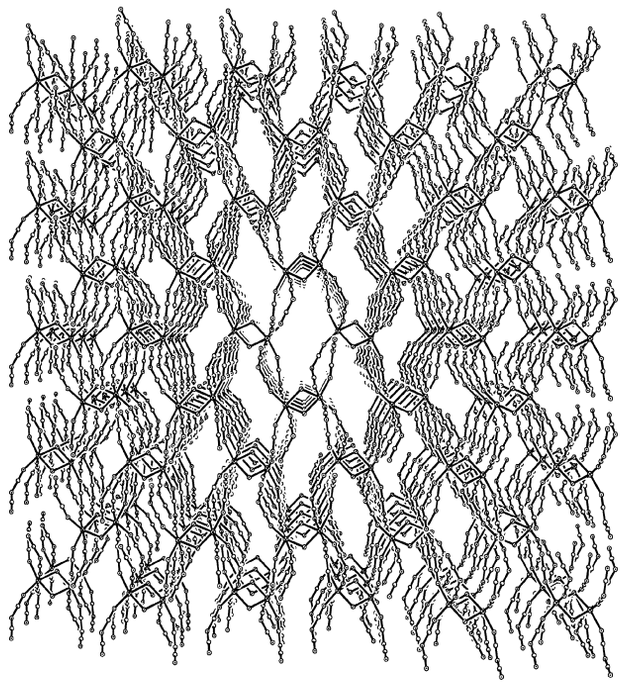

Fig. 2 Perspective view down the *a* axis of $[Co(apo)(N(CN)_2)_2]$ (2-aminopyridine has been omitted for clarity). The structures of complexes **2** and **3** are isomorphous.

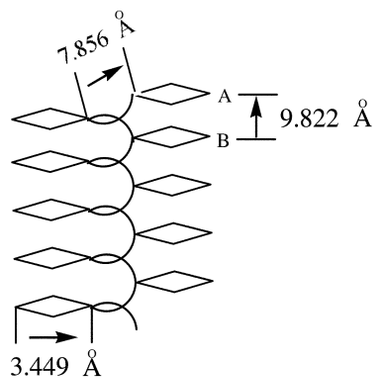

Fig. 3 Schematic view of complex **1** showing the helix linking of adjacent dimers with bridge NCNCN. ⌒ Stands for bridge NCNCN, ◇ for the dimer of the complex.

Co_2O_2 rhombic dimers.[11] The dicyanamide ligand possesses pseudo-C_{2v} symmetry with C≡N bond distances ranging from 1.135 to 1.147 Å. The packing of the complex along the *a* axis is shown in Fig. 2. The dihedral angle between the rhombic dimer plane and the ring of 2-aminopyridine is 88.83(7)°. The rhombic dimer planes are stacked along the *a* axis (see Fig. 2). Fig. 3 shows the helix linking of the adjacent dimers with $\mu_{1,5}$ $[N(CN)_2]^-$ bridges. The distance between rhombic dimer planes A and B is 9.822 Å, and that between two cobalt(II) atoms linked by $[N(CN)_2]^-$ is 7.856 Å.

Complexes $[Ni(apo)(N(CN)_2)_2]$ 2 and $[Mn(apo)(N(CN)_2)_2]$ 3

The structures of complexes **2** and **3** are very similar to that of $[Co(apo)(N(CN)_2)_2]$, and it is worthwhile to note that the intradimer distances between the two metal atoms Ni(1)···Ni(1A) and Mn(1)···Mn(1A) are 3.381(1) and 3.615(1) Å with bridge angles Ni(1)–O(1)–Ni(1A) and Mn(1)–O(1)–Mn(1A) 107.63(12) and 109.51(5)°, respectively. The dihedral angles between the rhombic dimer plane and the ring of 2-aminopyridine are 87.99(7) and 89.28(0.05)° for **2** and **3**, respectively. The distances between rhombic dimer planes A and B are 9.789, 9.866 Å, and between the two metal atoms linked by $[N(CN)_2]^-$ are 7.940, 7.925 Å for **2** and **3**, respectively.

Table 1 Crystallographic data for [Co(apo)(N(CN)$_2$)$_2$] **1**, [Ni(apo)(N(CN)$_2$)$_2$] **2** and [Mn(apo)(N(CN)$_2$)$_2$] **3**

	1	**2**	**3**
Formula	$C_9H_6CoN_8O$	$C_9H_6N_8NiO$	$C_9H_6MnN_8O$
M	301.15	300.93	297.16
Crystal system	Monoclinic	Monoclinic	Monoclinic
Space group	$P2_1/n$	$P2_1/n$	$P2_1/n$
a/Å	9.8222(3)	9.7889(5)	9.8655(3)
b/Å	11.8553(4)	11.7071(6)	12.1640(4)
c/Å	10.4718(4)	10.5283(4)	10.5046(3)
β/°	94.866(2)	94.610(3)	94.795(2)
V/Å^3	1214.99(7)	1202.64(10)	1256.18(7)
T/K	293(2)	293(2)	293(2)
Z	4	4	4
μ/cm^{-1}	1.418	1.619	1.056
Reflections collected	22597	21191	22515
Independent reflections	2879	2847	2970
R_{int} for equivalent reflections	0.0408	0.0780	0.0300
Final $R1$, $wR2$ [$I > 2\sigma(I)$]	0.0500, 0.1282	0.0594, 0.1377	0.0336, 0.0889

Table 2 Selected interatomic distances (Å) and angles (°) for [Co(apo)(N(CN)$_2$)$_2$] **1**

Co(1)–N(3)	2.074(2)	Co(1)–N(5B)	2.121(3)
Co(1)–N(6)	2.097(2)	Co(1)–N(8C)	2.134(2)
Co(1)–O(1A)	2.1140(18)	Co(1)–O(1)	2.1442(18)
O(1)–N(1)	1.343(3)	Co(1)···Co(1A)	3.4485(7)
N(7)–C(8)	1.312(4)	N(3)–C(6)	1.146(4)
N(8)–C(9)	1.144(4)	N(4)–C(7)	1.296(4)
N(4)–C(6)	1.301(4)	N(6)–C(8)	1.147(4)
N(5)–C(7)	1.135(4)	N(7)–C(9)	1.307(4)
N(3)–Co(1)–N(6)	105.21(11)	N(6)–Co(1)–N(5B)	88.82(11)
N(3)–Co(1)–O(1A)	163.39(9)	O(1A)–Co(1)–N(5B)	91.65(9)
N(6)–Co(1)–O(1A)	91.23(9)	N(3)–Co(1)–N(8C)	86.40(11)
N(3)–Co(1)–N(5B)	91.04(11)	N(6)–Co(1)–N(8C)	93.13(10)
O(1A)–Co(1)–N(8C)	90.43(9)	N(6)–Co(1)–O(1)	162.72(9)
N(5B)–Co(1)–N(8C)	177.12(10)	O(1A)–Co(1)–O(1)	71.84(7)
N(3)–Co(1)–O(1)	91.87(9)	N(5B)–Co(1)–O(1)	88.26(10)
N(8C)–Co(1)–O(1)	90.50(9)	N(1)–O(1)–Co(1)	125.89(15)
N(1)–O(1)–Co(1A)	123.89(16)	Co(1A)–O(1)–Co(1)	108.16(7)

Symmetry transformations used to generate equivalent atoms: A $-x$, $-y$, $-z+1$; B $-x-\frac{1}{2}$, $y-\frac{1}{2}$, $-z+\frac{1}{2}$; C $-x+\frac{1}{2}$, $y+\frac{1}{2}$, $-z+\frac{1}{2}$.

Table 3 Selected interatomic distances (Å) and angles (°) for [Ni(apo)(N(CN)$_2$)$_2$] **2**

Ni(1)–N(3)	2.043(4)	Ni(1)–N(5B)	2.077(4)
Ni(1)–N(6)	2.058(4)	Ni(1)–N(8C)	2.096(4)
Ni(1)–O(1A)	2.082(3)	Ni(1)–O(1)	2.107(3)
O(1)–N(1)	1.347(4)	O(1)–Ni(1A)	2.082(3)
N(3)–C(6)	1.144(6)	Ni(1)···Ni(1A)	3.381(1)
N(3)–Ni(1)–N(6)	101.98(16)	N(3)–Ni(1)–N(5B)	91.05(16)
N(3)–Ni(1)–O(1A)	165.55(14)	N(6)–Ni(1)–N(5B)	89.06(16)
N(6)–Ni(1)–O(1A)	92.29(13)	O(1A)–Ni(1)–N(5B)	91.47(14)
N(3)–Ni(1)–N(8C)	86.61(16)	N(5B)–Ni(1)–N(8C)	177.17(15)
N(6)–Ni(1)–N(8C)	92.99(16)	N(3)–Ni(1)–O(1)	93.52(14)
O(1A)–Ni(1)–N(8C)	90.40(13)	N(6)–Ni(1)–O(1)	164.23(13)
O(1A)–Ni(1)–O(1)	72.37(12)	N(1)–O(1)–Ni(1A)	123.7(2)
N(5B)–Ni(1)–O(1)	87.73(15)	N(1)–O(1)–Ni(1)	126.3(2)
N(8C)–Ni(1)–O(1)	90.81(13)	Ni(1A)–O(1)–Ni(1)	107.63(12)

Symmetry transformations as in Table 2.

Table 4 Bond lengths [Å] and angles [°] for [Mn(apo)(N(CN)$_2$)$_2$] **3**

Mn(1)–N(3)	2.170(2)	Mn(1)–N(5B)	2.224(2)
Mn(1)–N(6)	2.189(2)	Mn(1)–O(1)	2.225(1)
Mn(1)–O(1A)	2.201(1)	Mn(1)–N(8C)	2.238(2)
O(1)–N(1)	1.350(2)	N(1)–C(5)	1.362(3)
O(1)–Mn(1A)	2.201(1)	Mn(1)···Mn(1A)	3.615(1)
N(3)–Mn(1)–N(6)	107.86(8)	N(6)–Mn(1)–O(1)	160.88(7)
N(3)–Mn(1)–O(1A)	161.14(7)	O(1A)–Mn(1)–O(1)	70.49(5)
N(6)–Mn(1)–O(1A)	90.73(6)	N(5B)–Mn(1)–O(1)	87.99(7)
N(3)–Mn(1)–N(5B)	91.99(8)	N(3)–Mn(1)–N(8C)	86.42(8)
N(6)–Mn(1)–N(5B)	88.96(8)	N(6)–Mn(1)–N(8C)	93.57(8)
O(1A)–Mn(1)–N(5B)	91.43(7)	O(1A)–Mn(1)–N(8C)	89.40(6)
N(3)–Mn(1)–O(1)	91.10(7)	N(5B)–Mn(1)–N(8C)	177.32(8)
Mn(1A)–O(1)–Mn(1)	109.51(5)	O(1)–Mn(1)–N(8C)	89.89(7)

Symmetry transformations as in Table 2.

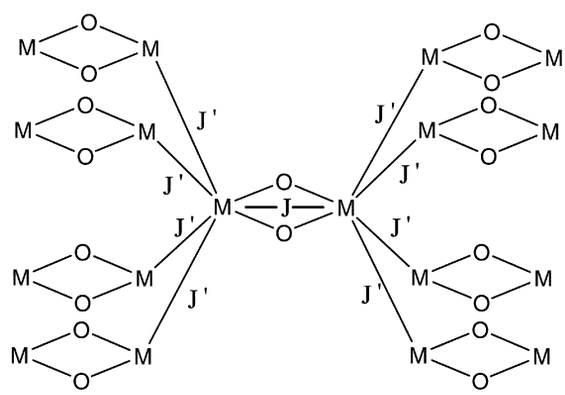

Fig. 4 Scheme of the exchange pathways for the [M(apo)(N(CN)$_2$)$_2$] with the coupling constants.

Magnetochemistry

The exchange pathways in these complexes with dimer skeletons can be schematized as shown in Fig. 4, where J stands for the intradimer interaction parameter and J' for the interdimer interaction parameter. The temperature dependences of the magnetic susceptibilities are shown in Fig. 5, in the form of χ_m *vs.* T (a) and $\chi_m T$ *vs.* T plots (b), χ_m being the corrected molar magnetic susceptibility per dimer unit. Maximum peaks (T_{max}) observed in the χ_m *vs.* T curves indicated an antiferromagnetic (AF) exchange, and the positions of the peaks suggested that the magnitude of the AF interactions decreased in the following order: **2** (T_{max} = 100 K) > **1** (50) > **3** (15).

The $\chi_m T$ value of complex **1** exhibits a continuous decrease upon cooling. The value per cobalt(II) dimer at room temperature (5.2 cm^3 K mol^{-1}) is larger than that calculated for the spin-only case (3.75 cm^3 K mol^{-1}), revealing a significant orbital contribution as also frequently observed in other cobalt(II) complexes. It is very difficult to estimate the exchange interaction accurately within cobalt(II) complexes because of the effects of spin–orbit coupling. In this paper the model is an admittedly simple one, just considering the orbital contribution to an assumed isotropic g parameter,[12] wherein the temperature dependence of the magnetic susceptibility for **1** is assumed to be due mainly to intradimer exchange interaction (J) and interdimer exchange interaction (J'). Since the distance between two

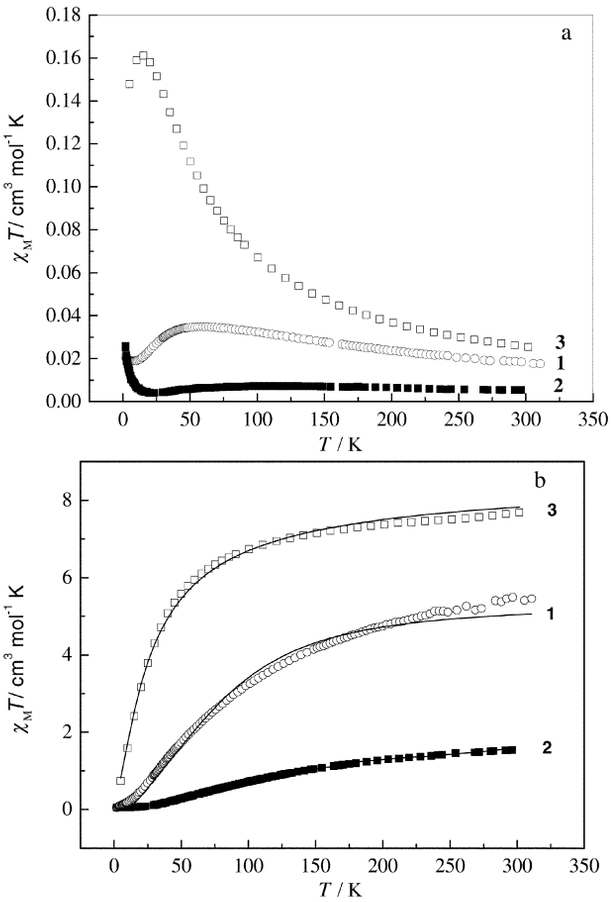

Fig. 5 Temperature dependence of the χ_m (a) and $\chi_m T$ (b) of $[M(apo)(N(CN)_2)_2]$ **1**, **2** and **3**. The solid lines represent the best fit curves.

Co^{II} linked by $[N(CN)_2]^-$ is considerably longer (7.86 Å) compared with the intradimer Co1···Co1A (3.45 Å) separation, the interdimer exchange interactions (J') can be seen further approximately as the effect of the molecular field. So the susceptibility (χ) of **1** is given as eqn. (1), where z is the number

$$\chi = \frac{\chi_{dimer}}{[1 - (2zJ'/N\beta^2 g^2)\chi_{dimer}]} \quad (1)$$

of nearest neighbors of the dimers (8 in this case) and $x = J/kT$. Eqn. (1) has been modified to (3) to include the

$$\chi_{dimer} = \frac{2N\beta^2 g^2}{kT}\left[\frac{e^{-10x} + 5e^{-6x} + 14}{e^{-12x} + 3e^{-10x} + 5e^{-6x} + 7}\right] \quad (2)$$

$$\chi_m = \chi(1 - \rho) + [\rho N\beta^2 g^2 S(S + 1)/3kT] + 2N_\alpha \quad (3)$$

contribution of the uncoupled impurity species (mole fraction, ρ), assumed to follow a Curie law, and temperature-independent paramagnetism (N_α); N, β, g, k, and T have their usual meanings. Non-linear least-squares fittings of the theoretical expression to the experimental data have been made by varying J, J', g, and ρ and minimizing the residual $R = [\Sigma(\chi_{obs}T - \chi_{calc}T)^2/\Sigma(\chi_{obs}T)^2]$.

The best fit of eqn. (3) to the data was achieved with $J = -17.8$ cm^{-1}, $J' = 2.7$ cm^{-1}, $g = 2.38$, $\rho = 0.004$, $R = 2.3 \times 10^{-3}$. It seems that the spin-only model gives quite a good fit, probably because the orbital effect is partly accommodated in the larger g parameter.

The $\chi_m T$ value per nickel(II) dimer **2** decreases with decreasing temperature from 1.58 (300) to 0.052 cm^3 K mol^{-1} (2 K). Such behavior is indicative of an antiferromagnetic coupling. As far as we know, there is no exact mathematical expression to evaluate the susceptibility of such a 3-D system (Fig. 4). Thus, the dimer model of Ginsberg *et al.*[13] was used, with eqn. (5) described by the Hamiltonian (4) which includes zero-field splitting (D), the usual intradimer exchange (J), and also an interdimer exchange parameter (J'); N_α is taken as 200×10^{-6}

$$H = -2J\hat{S}_1\hat{S}_2 - D(\hat{S}_1^2 + \hat{S}_2^2) - 16J'\hat{S}_i\langle\hat{S}_i\rangle - g_i\beta\hat{H}\hat{S}_i \quad (4)$$

$$\chi_m = \chi(g, J, D, J')(1 - \rho) + (2N\beta^2 g^2\rho/3kT) + 2N_\alpha \quad (5)$$

$$\chi(g, J, D, J') = \frac{Ng^2\beta^2}{3k}\left(\frac{F_1(J, D, T)}{T - 16J'F_1(J, D, T)} + \frac{2F'(J, D, T)}{1 - 16J'F'(J, D, T)}\right) \quad (6)$$

$$F'(J, D, T) = \frac{1}{D}F_2(J, D, T) + \frac{3C_2^2}{3J - \delta}F_3(J, D, T) + \frac{3C_1^2}{3J + \delta}F_4(J, D, T) \quad (7)$$

$$F_1(J, D, T) = \frac{1 + e^{4J/kT} + 4e^{4J/kT}e^{D/kT}}{2 + e^{D/kT} + e^{J/kT}e^{-\delta/kT} + e^{J/kT}e^{\delta/kT} + 2e^{4J/kT} + 2e^{4J/kT}e^{D/kT}} \quad (8)$$

$$F_2(J, D, T) = \frac{2e^{4J/kT}e^{D/kT} + e^{D/kT} - 1 - 2e^{4J/kT}}{2 + e^{D/kT} + e^{J/kT}e^{-\delta/kT} + e^{J/kT}e^{\delta/kT} + 2e^{4J/kT} + 2e^{4J/kT}e^{D/kT}} \quad (9)$$

$$F_3(J, D, T) = \frac{e^{4J/kT} - e^{J/kT}e^{\delta/kT}}{2 + e^{D/kT} + e^{J/kT}e^{-\delta/kT} + e^{J/kT}e^{\delta/kT} + 2e^{4J/kT} + 2e^{4J/kT}e^{D/kT}} \quad (10)$$

$$F_4(J, D, T) = \frac{e^{4J/kT} - e^{J/kT}e^{-\delta/kT}}{2 + e^{D/kT} + e^{J/kT}e^{-\delta/kT} + e^{J/kT}e^{\delta/kT} + 2e^{4J/kT} + 2e^{4J/kT}e^{D/kT}} \quad (11)$$

$$\delta = [(3J + D)^2 - 8JD]^{1/2} \quad (12)$$

$$C_1 = 2.828D/[(9J - D + 3\delta)^2 + 8D^2]^{1/2} \quad (13)$$

$$C_2 = (9J - D + 3\delta)/[(9J - D + 3\delta)^2 + 8D^2]^{1/2} \quad (14)$$

cm^3 mol^{-1} per Ni^{II}. The best-fit parameters obtained from minimizing R were $J = -40$ cm^{-1}, $J' = 1.51$ cm^{-1}, $D = 18$ cm^{-1}, $g = 2.23$, $\rho = 0.012$, and $R = 4.3 \times 10^{-4}$. The g value is also in accord with expectation for nickel(II).[14] Nag and co-workers have shown that the value of $-J$ increases linearly with increase of the $Ni–O_{(Phenoxy)}$–Ni bridge angle or intramolecular Ni···Ni separation in μ-O-bridged dinickel(II) complexes.[15] This is quite similar to the correlation found by Hatfield and co-workers for hydroxy-bridged dinuclear copper(II) complexes, which is one of the most useful and best known magneto-structural correlations.[16] Our results are compared with the early reported values for similar Ni_2O_2 types of complexes in Table 5. The magnetic parameters of the complex $[Ni(apo)(N(CN)_2)_2]$ resulting from the least-squares fits are in accord with expectation for nickel(II) dimer complexes, although they do not strictly obey Nag's linear relationship. This deviation may be due to the difference between the bridging *N*-oxide and phenoxy oxygen atoms.

The $\chi_m T$ *vs.* T plots for complex **3** in the 4–300 K range are also shown in Fig. 5(b). The $\chi_m T$ value per manganese(II) dimer decreases gradually with decreasing temperature, indicating the presence of an antiferromagnetic exchange interaction. The

Table 5 Magnetic and structure parameters for some nickel dimer complexes

Complex	Ni · · · Ni/Å	Ni–O–Ni/°	J/cm^{-1}	g	J'/cm^{-1}	D/cm^{-1}	Reference
$[Ni_2(Damox)_2(py)_4]\cdot 2py$ [a]	3.058	96.9	−19.5	2.16	−2.33	15.82	17
$[Ni_2L(NCS)_2(H_2O)_2]\cdot 2Me_2NCHO$ [b]	3.105	99.2	−21.3	2.19	2.0	1.9	18
$[Ni_2L(MeOH)_2(ClO_4)_2]\cdot 2NHEt_3ClO_4$ [b]	3.135	101.3	−29.5	2.29	−4.7	29.9	18
$[Ni_2L(py)_2][ClO_4]_2$ [b]	3.206	105.7	−67.1	2.24	6.9	22.8	18
$[Ni(apo)(N(CN)_2)_2]$	3.3807	107.63	−40	2.23	1.51	18	This work

[a] H_2Damox = 2,6-bis(acetoximato)-4-methylphenol. [b] H_2L = 10,21-Dimethyl-3,6,14,17-tetraazacyclotetracosa-1(23),2,6,8(24),9,11,13,17,19,21,23,24-diol.

$$\chi_{\text{dimer}} = \frac{2Ng^2\beta^2}{kT}\left[\frac{55 + 30\exp(-10J/kT) + 14\exp(-18J/kT) + 5\exp(-24J/kT) + \exp(-28J/kT)}{11 + 9\exp(-10J/kT) + 7\exp(-18J/kT) + 5\exp(-24J/kT) + 3\exp(-28J/kT) + \exp(-30J/kT)}\right] \quad (16)$$

theoretical susceptibility equation resulting from consideration of both isotropic intradimer exchange (J) and interdimer exchange (J') in the molecular field approximation affords a reasonable fit [eqn. (15)]. Single-ion zero-field interactions DS_z^2

$$\chi_{\text{m}} = \frac{\chi_{\text{dimer}}}{[1 - (2zJ'/N\beta^2g^2)\chi_{\text{dimer}}]} \quad (15)$$

were not taken into account in our theoretical susceptibility equation.[13] The parameters obtained from that fit are $J = -1.32$ cm^{-1}, $J' = -0.18$ cm^{-1}, $g = 1.98$ and $R = 2.6 \times 10^{-4}$. It should be noted that weak anti- and ferro-magnetic exchange interactions for other dimer manganese(II) systems have been reported. The proposed diphenoxy-bridged dimer $[Mn(SALPS)]_2$ [19] {SALPS = *N*,*N*′-[1,1′-dithiobis(phenylene)]bis(salicylideneaminato)} has $J = -1.88$ cm^{-1}, $[Mn(SALEN)]_2$ [20,21] has $J = -6.5$ cm^{-1} and $[Mn(OC_6X_3H_2)_2(bpy)]_2$ (X = Cl or Br) has $J = +0.74$ and $+2.25$ cm^{-1}, respectively.[22] There appears to be no simple relation between the magnetism and observed Mn–O–Mn angles.

The order of the J_{intra} value resulting from the least-squares fits of the three complexes is $|J_{\text{NiNi}}| > |J_{\text{CoCo}}| > |J_{\text{MnMn}}|$, in accord with the positions of the maximum peaks in χ_{m} *vs.* T curves. In the simplest treatment of intradimer interaction only the SOMOs (singly occupied molecular orbitals) are considered. The exchange interaction parameter $J_{\text{MM}'}$ is expressed by means of the individual interactions J_{ij} as in eqn. (17) where n_i and

$$J_{\text{MM}'} = J_{\text{AF}} + J_{\text{F}} = \frac{1}{n_i n_j}\sum_{ij} J_{ij} \quad (17)$$

n_j are the numbers of unpaired electrons on metal ions M and M′. The nickel(II) ion under O_h symmetry has two unpaired electrons on the e_g ($d_{x^2-y^2}$, d_{z^2}) orbitals. The overall exchange integral J_{NiNi} is (1/4)[$J_{x^2-y^2,\ x^2-y^2} + 2J_{x^2-y^2,\ z^2} + J_{z^2,\ z^2}$], where the $J_{x^2-y^2,\ z^2}$ component is positive (J_{F}) due to the orthogonality of the magnetic orbitals. On the contrary, $J_{x^2-y^2,\ x^2-y^2}$ and $J_{z^2,\ z^2}$ (J_{AF}) produce an antiferromagnetic contribution to the overall exchange integral. Since $|J_{\text{AF}}|$ is larger than $|J_{\text{F}}|$ in the nickel(II) dimer, the net exchange integral J_{NiNi} is negative (−40 cm^{-1}). Comparing J_{NiNi} with J_{CoCo} and J_{MnMn}, it appears that the relative predominance of the antiferromagnetic contribution tends to weaken with increasing unpaired electrons in the metal(II) t_{2g} orbital.[23]

In conclusion we have synthesized three novel 3-D coordination polymers constructed by dimer subunits, intradimerly bridged by *N*-oxide oxygens and interdimerly bridged by $\mu_{1,5}$-NCNCN. The values for the intradimer spin coupling constant J were estimated to be −17.8, −40 and −1.3 cm^{-1} for **1**–**3**, respectively.

Acknowledgements

We acknowledge financial support from the National Natural Science Foundation of China (No. 29771001 and 29831010), the National Key Project Fundamental Research (G199806-1306), and the Excellent Young Teachers Fund of MOE, P. R. China.

References

1 J. L. Manson, A. M. Arif and J. S. Miller, *J. Mater. Chem.*, 1999, **9**, 979.
2 S. R. Batten, P. Jensen, B. Moubaraki, K. S. Murray and R. Robson, *Chem. Commun.*, 1998, 439.
3 M. Kurmoo and C. J. Kepert, *New J. Chem.*, 1998, 1515.
4 J. L. Manson, C. R. Kmety, Q. Z. Huang, J. W. Lynn, G. M. Bendele, S. Pagola, P. W. Stephens, L. M. Liable-Sands, A. L. Rheingold, A. J. Epstein and J. S. Mill, *Chem. Mater.*, 1998, **10**, 2552.
5 S. R. Batten, P. Jensen, C. J. Kepert, M. Kurmoo, B. Moubaraki, K. S. Murray and D. J. Price, *Chem. Commun.*, 1999, 177.
6 P. Jensen, S. R. Batten, G. D. Fallon, B. Moubaraki, K. S. Murray and D. J. Price, *J. Solid State Chem.*, 1999, **145**, 369.
7 P. Jensen, S. R. Batten, G. D. Fallon, D. C. R. Hockless, B. Moubaraki, K. S. Murray and R. Robson, *J. Solid State Chem.*, 1999, **145**, 387.
8 S. S.-Y. Chui, S. M.-F. Lo, J. P. H. Charmant, A. G. Orpen and I. D. Williams, *Science*, 1999, **283**, 1148.
9 G. M. Sheldrick, SHELXL 97, Program for crystal structure refinement, University of Göttingen, 1997.
10 C. K. Johnson, ORTEP II, Report ORNL-5138, Oak Ridge National Laboratory, Oak Ridge, TN, 1976.
11 D. C. Craig, D. J. Phillips and F. M. Z. Kaifi, *Inorg. Chim. Acta*, 1989, **161**, 247.
12 P. W. Ball and A. B. Blake, *J. Chem. Soc. A*, 1969, 1415.
13 A. P. Ginsberg, R. L. Martin, R. W. Brookes and R. C. Sherwood, *Inorg. Chem.*, 1972, **11**, 2884.
14 J. E. Wertz and J. R. Bolton, *Electron Spin Resonance: Elementary Theory and Practical Applications*, McGraw-Hill Book Co., New York, 1972.
15 K. K. Nanda, L. K. Thompson, J. N. Bridson and K. Nag, *J. Chem. Soc.*, *Chem. Commun.*, 1994, 1337.
16 V. M. Crawford, M. W. Richardson, J. R. Wasson, D. J. Hodgson and W. E. Hatfield, *Inorg. Chem.*, 1976, **15**, 2107.
17 K. K. Nanda, A. W. Addison, N. Paterson, E. Sinn, L. K. Thompson and U. Sakaguchi, *Inorg. Chem.*, 1998, **37**, 1028.
18 K. K. Nanda, R. Das, L. K. Thompson, K. Venkatsubramanian, P. Paul and K. Nag, *Inorg. Chem.*, 1994, **33**, 1188.
19 D. D. Kessissoglou, W. M. Butler and V. L. Pecoraro, *Inorg. Chem.*, 1987, **26**, 495.
20 A. Earnshaw, E. A. King and L. F. Larknorthy, *J. Chem. Soc. A*, 1968, 1048.
21 B. J. Kennedy and K. S. Murray, *Inorg. Chem.*, 1985, **24**, 1552.
22 M. Wesolek, D. Meyer, J. A. Osborn, A. D. Cian, J. Sischer, A. Derory, P. Legoll and M. Drillon, *Angew. Chem.*, *Int. Ed. Engl.*, 1994, **33**, 1592.
23 P. W. Ball and A. B. Blake, *J. Chem. Soc.*, *Dalton Trans.*, 1974, 853.